Deep-Sea Research, Vol. 39. No. 2. pp. 235–244. 1992.
Printed in Great Britain.

0198–0149/92 $5.00 + 0.00

Growth rates of ferromanganese encrustations on rocks from the Romanche Fracture Zone, Equatorial Atlantic

ERIC O. ODADA*

(*Received* 7 *March* 1991; *in revised form* 1 *April* 1991; *accepted* 2 *April* 1991)

Abstract—Based on radiochemical techniques, ferromanganese oxide crusts from the Romanche Fracture Zone (RFZ) have accretion rates ranging between 1.4 and 2.8 mm/10^6 years. In comparison with other ferromanganese deposits, the accretion rates for the RFZ crusts are close to the growth rates for typical hydrogenetic deposits formed on elevations and exposed rock surfaces in the Pacific Ocean. This would suggest that the RFZ crusts are formed by slow accumulation of metal hydroxides from the water column, probably in a manner analogous to the Pacific seamount crusts.

INTRODUCTION

FERROMANGANESE oxide deposits are more scarce in the Atlantic than in the Pacific and Indian Oceans, probably due to the generally higher sedimentation rates in the Atlantic (CRONAN, 1977; ODADA, 1990a). Two types of ferromanganese encrustations, however, have been recovered in moderate abundance (AUMENTO *et al.*, 1968; SCOTT *et al.*, 1974; CRONAN, 1977; HOFFERT *et al.*, 1978; GODDARD *et al.*, 1987). One is associated with submarine volcanic activity and the other is formed by hydrogenous precipitation, i.e. direct precipitation or accumulation of colloidal metal oxides from seawater.

In this study, a suite of ferromanganese oxide crusts dredged from a wide variety of depths within the Romanche Fracture Zone (RFZ; Table 1) were studied by radiochemical techniques to determine their rates of accretion. The rates of accretion can be determined either by dating the nuclei around which ferromanganese oxide layers accumulate or by assessing age differences of successive layers (KU, 1977). The nucleus dating approach gives only the maximum age at which the first oxide layers begin to form (FINNEY *et al.*, 1984). The second approach assumes that radioactive nuclides are incorporated into the oxide layers at a constant rate as they are deposited. This latter approach is preferred for dating crusts without nuclei and was adopted in this work.

SAMPLE LOCATIONS AND DESCRIPTION

Ferromanganese crusts and associated substrate material were dredged from the RFZ by R.R.S. *Shackleton* in 1983. Additional samples were obtained from Laboratoire mixte CNRS-CEA (Gif-sur-Yvette, France). Station details and crust descriptions are given in

*Department of Geology, University of Nairobi, P.O. Box 30197, Nairobi, Kenya.

Table 1. *Station details and crust descriptions*

Station no.	Position	Depth (m)	Crust description
SH2-35	0°21.0′N; 18°30.0′W	4700–5000	Crust less than 1 cm thick. No substrate attached. Surface irregular and cavernous, orange to black in colour.
SH2-48	0°22.7′S; 18°24.7′W	2739–2850	Encrustation less than 2 mm around altered volcanic rocks.
SH2-59	0°33.1′N; 16°20.9′W	1869–1880	Crusts of thicker than 1 cm coating of small irregular pieces of altered volcanic rock, mostly basalt. Surfaces are generally smooth and botryoidal.
CH-01	0°03.0′N; 18°32.0′W	3640–3250	Crusts of thicker than 1 cm coating of altered rock. They have knobbly outer surfaces with gritty texture and dark brown colour.
CH-03	0°02.1′S; 18°29.5′W	4300–4010	Crust coating of highly altered basaltic rock. The surface is knobbly with a gritty appearance. The colour is black.
CH-04	0°04.1′S; 18°28.2′W	4545–4040	Encrustation 1 mm or less around a piece of highly altered basalt. The colour of the crust is black and the surface has a smooth to coarsely granular texture.
CH-06	0°01.0′S; 18°27.0′W	3660–3580	Thin crust on highly altered breciated volcanic rock. The outer surface of the crust is knobbly with gritty texture. The colour is brownish with some yellowish-green streaks.
CH-07	0°03.8′N; 18°31.1′W	3300–2820	Thick crust with smooth, shiny surface and brownish colour. Some concentric banding is noticeable inside. No substrate attached.
CH-08	0°01.5′S; 18°30.1′W	4100–3500	Crust thicker than 1 cm over a yellowish-brown and highly altered volcanic rock, knobbly on the outer surface with a rough gritty texture.
CH-10	0°05.2′S; 18°29.0′W	4970–4650	Crust over 1 cm thick on basalt. The crust is slightly concentrically banded. The surface is smooth with granular texture.

Table 1. Two predominant morphological types of crust are common (Figs 1 and 2): (1) those showing a knobbly to botryoidal surface texture and a massive internal structure, commonly impregnated by sediments; (2) crusts displaying predominantly smooth to microgranular surface texture; these are more compact and show no impregnation by sediments.

MINERALOGY AND COMPOSITION

The salient features of the mineralogy and chemical variability of selected RFZ crusts are shown in Table 2. Crust SH2-35 exhibits a very different chemistry and mineralogy to the other crusts. Firstly, it is enriched in Fe and depleted in Mn, Co and Ni relative to the other crusts. Secondly, it is the only crust to contain goethite, although hydrogenous goethite-rich deposits from the Atlantic have been reported by MOORBY and CRONAN (1981). The remaining crusts have a mineralogy typical of hydrogenous crusts from the

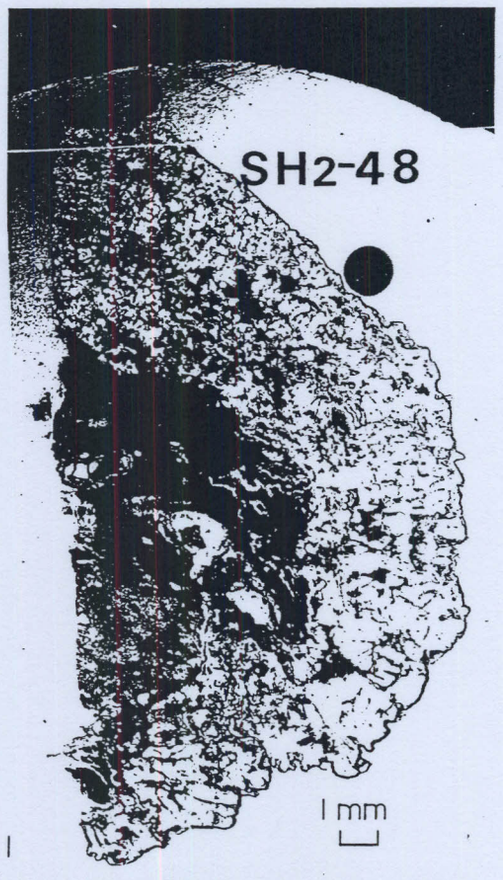

Fig. 1. Sample SH2-48, showing crust morphology.

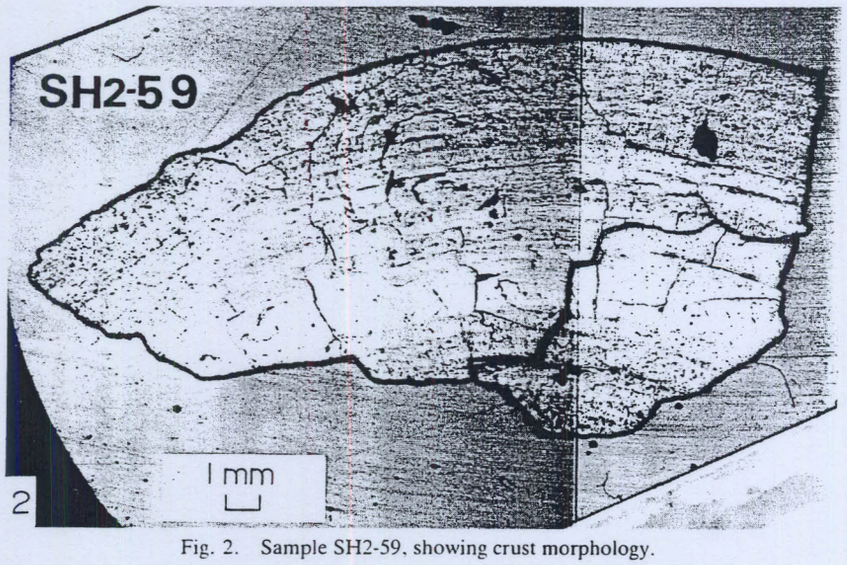

Fig. 2. Sample SH2-59, showing crust morphology.

Table 2. Mineralogy and composition of selected RFZ crusts (from ODADA, 1990*b*)

Sample no.	Mineralogy (XRD)	Water depth (m)	Ca (%)	Al (%)	Mn (%)	Fe (%)	Co (ppm)	Ni (ppm)	Mn/Fe ratio
SH2-59	S-MnO_2	1869–1880	2.5	0.8	19.5	17	9300	2900	1.1
SH2-48	S-MnO_2 + calcite + felspar	2850–2860	3.9	1.2	15.7	21	3400	2300	0.7
SH2-35	Poorly crystalline Fe oxide (goethite)	4700–5000	0.6	2.0	2.1	34	340	388	0.06

Line Islands Archipelago, central Pacific Ocean (APLIN and CRONAN, 1985) in that they are largely composed of S-MnO_2 and have a Mn/Fe ratio near unity.

The mean chemical composition of the RFZ crusts, excluding SH2-35, bears no similarity to either hydrothermal or diagenetic deposits, but is similar to hydrogenous crusts. The mean Mn/Fe ratio for the RFZ crusts is low in comparison with other hydrogenous crusts, particularly in relation to other crust varieties.

ANALYTICAL TECHNIQUE

Radiochemical analyses were run on the two different crusts at the Centre des Faibles Radioactivités, Laboratoire mixte CNRS-CEA (Gif-sur-Yvette, France), using the ^{230}Th and ^{231}Pa method described by KU and BROECKER (1969). Thin layers were scraped from the crust samples and totally dissolved in a mixture of hydrofluoric, perchloric, hydrochloric and nitric acids to dissolve silicates and other more resistant phases. The solutions were spiked with ^{232}U and ^{228}Th tracers in sufficient quantities to give about twice as much spike activity as natural ^{238}U or ^{232}Th, and then passed through a series of hydroxide precipitation, ion exchange and solvent extraction processes before uranium and thorium isotopes were finally electroplated onto stainless steel. Thorium and uranium isotopes were counted by alpha spectrometry using a surface-barrier solid-state detector and a multi-channel analyser. Protactinium was measured through ^{227}Th; the two are in secular equilibrium (THOMPSON, 1982).

RESULTS

The accretion rates in the ferromanganese oxide crusts were determined from the depth gradients of excess ^{230}Th and ^{227}Th (Tables 3 and 4; Figs 3 and 4). They are based on the assumption that the supply of these two isotopes and the bulk material to an accreting surface remains constant with time, and that ^{230}Th and ^{227}Th are immobile once deposited (MOORE *et al.*, 1981). The other assumption is that normal uranium content in the crust is in equilibrium with its daughter products in the radioactive decay series,

$$^{234}U = {}^{230}Th \text{ and } {}^{235}U = {}^{231}Pa = {}^{227}Th.$$

In addition to these isotopes, the ^{230}Th and ^{227}Th present in the water column are transferred to the crusts by scavenging as uranium-unsupported or excess ^{230}Th and ^{227}Th.

Table 3. Radiochemical data for crust SH2-48

Depth 1/10 mm	^{232}Th (dpm g^{-1})	^{230}Th (dpm g^{-1})	^{227}Th (dpm g^{-1})	^{234}U (dpm g^{-1})	$^{230}Th_{ex.}$* (dpm g^{-1})	$\frac{^{234}U}{^{238}U}$	$^{227}Th_{ex.}$† (dpm g^{-1})
0.0–0.30	14.0 ± 0.5	360 ± 20	77 ± 8	10 ± 2	350 ± 20	1.11 ± 0.09	76 ± 8
0.30–0.83	16.0 ± 1.0	322 ± 20	67 ± 7	10.1 ± 1.5	311 ± 21	1.16 ± 0.11	66 ± 7
0.83–1.77	13.6 ± 0.7	210 ± 15	32 ± 3	12.1 ± 2.0	198 ± 15	1.02 ± 0.12	31.5 ± 3.0
1.77–2.83	15.8 ± 0.9	153 ± 12	18 ± 3	11.1 ± 0.5	142 ± 12	1.05 ± 0.29	17.5 ± 3
2.83–4.45	14.2 ± 0.7	88 ± 10	7 ± 1	10.7 ± 1.1	77 ± 10	0.93 ± 0.06	6.5 ± 10
4.45–5.77	15.9 ± 0.9	59 ± 6	NM	11.8 ± 1.2	47 ± 6	1.02 ± 0.07	NM
5.8–7.4	13.2 ± 0.8	43 ± 5	NM	10.1 ± 1.3	33 ± 5	1.05 ± 0.07	NM
7.4–8.8	13.0 ± 1.4	27 ± 3	NM	10.2 ± 1.1	17 ± 3	1.03 ± 0.06	NM

NM = not measured.
*$^{230}Th_{ex.}$ = excess $^{230}Th = {}^{230}Th - {}^{234}U$.
†$^{227}Th_{ex.}$ = excess $^{227}Th = {}^{227}Th - 0.046\ {}^{238}U$.

Assuming that ^{230}Th is in radioactive equilibrium with ^{234}U, the excess activity can be derived as follows:

$$^{230}Th_{ex.} = {}^{230}Th - {}^{234}U.$$

The calculation of ^{227}Th is more complicated because ^{235}U is not measured but derived from ^{238}U as follows:

$$^{227}Th_{ex.} = {}^{227}Th - 0.046/{}^{238}U.$$

Table 4. Radiochemical data for crust SH2-59

Depth 1/10 mm	^{232}Th (dpm g^{-1})	^{230}Th (dpm g^{-1})	^{227}Th (dpm g^{-1})	^{234}U (dpm g^{-1})	$^{230}Th_{ex.}$* (dpm g^{-1})	$\frac{^{234}U}{^{238}U}$	$^{227}Th_{ex.}$† (dpm g^{-1})
0.0–0.28	27.1 ± 2.1	492 ± 20	110 ± 8	13.5 ± 2.1	479.20	1.10 ± 0.12	109 ± 8
0.0–0.50	30.0 ± 3.0	531 ± 40	114 ± 7	NM	518 ± 40‡	—	113 ± 7
0.28–0.74	25.3 ± 1.8	242 ± 15	52 ± 5	12.5 ± 2.0	229 ± 15	1.11 ± 0.10	51 ± 5
0.50–1.10	22.4 ± 2.1	230 ± 25	56 ± 5	NM	217 ± 25‡	—	56 ± 5
0.74–1.26	22.1 ± 2.4	217 ± 6	21.2 ± 3.8	15.1 ± 2.1	112 ± 7	1.03 ± 0.07	20.6 ± 4.0
1.10–1.60	25.3 ± 2.5	159 ± 16	25.9 ± 2.9	NM	146 ± 16‡	—	25.2 ± 3.0
1.26–1.92	21.7 ± 1.9	86.5 ± 3.1	11.7 ± 2.1	13.9 ± 1.1	72.6 ± 3.2	1.07 ± 0.07	11.0 ± 2.4
1.92–2.45	22.6 ± 2.1	68.2 ± 7.1	8.2 ± 2.1	12.6 ± 2.1	55.6 ± 7.3	1.00 ± 0.10	7.6 ± 2.8
2.45–3.20	20.6 ± 2.0	46.1 ± 4.2	3.6 ± 1.2	14.0 ± 1.1	32.1 ± 4.3	1.08 ± 0.07	3.0 ± 1.6
3.20–3.74	19.0 ± 2.1	35.2 ± 4.3	2.7 ± 1.0	12.9 ± 0.9	22.3 ± 4.4	1.11 ± 0.07	2.1 ± 1.3
3.74–4.34	19.0 ± 2.0	27.1 ± 3.0	1.9 ± 0.4	13.0 ± 1.1	14.1 ± 3.2	0.97 ± 0.07	1.3 ± 1.2
5.40–6.40	19.1 ± 1.2	17.7 ± 1.1	NM	13.2 ± 1.1	4.5 ± 1.6	0.95 ± 0.05	NM
8.50–10.40	16.3 ± 0.8	14.8 ± 0.8	NM	14.0 ± 1.2	0.8 ± 0.9	1.02 ± 0.07	NM
110–130	13.7 ± 0.5	12.2 ± 0.4	NM	13.9 ± 0.4	—	0.97 ± 0.04	NM

NM = not measured.
*$^{230}Th_{ex.}$ = excess $^{230}Th = {}^{230}Th - {}^{234}U$.
†$^{227}Th_{ex.}$ = excess $^{227}Th = 0.046\ {}^{238}U$.
‡Estimated values using an average value of 13.5 for ^{234}U.

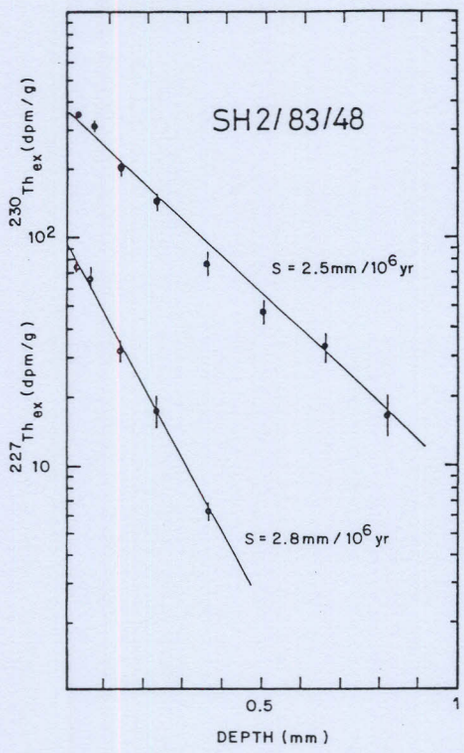

Fig. 3. ^{230}Th and ^{227}Th (dpm g^{-1}) activities as a function of depth in crust SH2-48.

DISCUSSION

The radiometric dates presented in this work provide information on the mode of accretion of the RFZ crusts. As can be seen in Fig. 4, crust SH2-59 exhibits very low isotopic activity in the near-surface layers, making it difficult to determine accurately the ratio in which thorium and protactinium (or ^{227}Th) were incorporated. In part this may be due to laboratory contamination associated with the sampling procedure, as the peeling of layers may not have completely removed single growth surfaces, and partly due to the infiltration of younger material along cracks or fissures in the crust (Fig. 2).

The measured accretion rates for crust SH2-48 range between 2.5 and 2.8 mm/10^6 years and for crust SH2-59 between 1.4 and 2.0 mm/10^6 years (Figs 3 and 4). These rates of accretion for the RFZ crusts are close to those of hydrogenetic deposits formed in the Pacific Ocean where sediments do not interact with the accretion of the deposits (Table 5). This suggests that the RFZ crusts have accreted through a similar process, i.e. from a hydrogenous source.

Most studies on ferromanganese nodules and crusts based on radiochemical analyses of nuclei or the surrounding oxyhydroxide layers (KU, 1977; LYLE *et al.*, 1977; DYMOND *et al.*, 1984; FINNEY *et al.*, 1984; REYSS *et al.*, 1985) have shown that hydrothermal and diagenetic accretion are generally two orders of magnitude faster (100–200 mm/10^6 years) than hydrogenous accretionary rates (Table 5; DYMOND *et al.*, 1984).

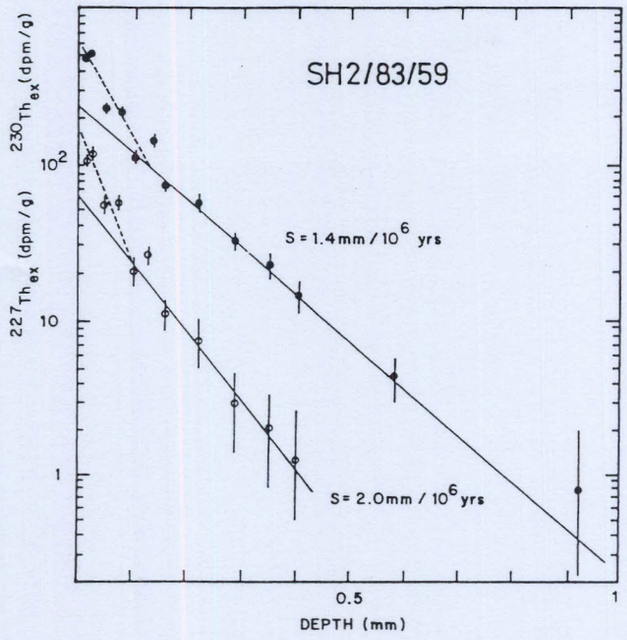

Fig. 4. ^{230}Th and ^{227}Th (dpm g^{-1}) activities as a function of depth in crust SH2-59.

The geochemical data for the RFZ sediment samples (ODADA, 1990a) and the ferromanganese encrustations (ODADA, 1990b) indicate that the concentration of metals in these deposits can be accounted for in terms of biogenic, detrital and authigenic contributions from hydrogenous and diagenetic sources. The hydrogenous source is important only where bulk sedimentation rate is low, whilst the diagenetic source is significant where

Table 5. Growth rates of the RFZ crusts and other Fe–Mn deposits from different areas

Sample reference	Growth rates (mm/10^6 y)	Data source
RFZ crusts SH2-48	2.5–2.8	This study
RFZ crusts SH2-59	1.4–2.0	This study
Seamount crusts (hydrogenous)	0.8–2.7	HALBACH *et al.* (1983)
Wahine nodules (diagenetic)	4.7–11.0	HALBACH *et al.* (1983)
MANOP sites H, S, R, nodules (hydrogenous)	1.0–2.0	DYMOND *et al.* (1984)
MANOP sites H, S, R, nodules (oxic diagenesis)	10–50	DYMOND *et al.* (1984)
MANOP sites H, S, R, nodules (suboxic diagenesis)	100–200	DYMOND *et al.* (1984)
MAR crusts (hydrothermal)	100–200	SCOTT *et al.* (1974)
MANOP site H (diagenetic)	30–300	FINNEY *et al.* (1984)
Central Pacific crusts (hydrogenous)	2.7–4.8	SEGL *et al.* (1984)
Peru Basin nodules (diagenetic,	200	REYSS *et al.* (1984)
hydrogenous)	6	REYSS *et al.* (1984)

reducing conditions occur within the sediments. Investigations of the inter-element relationships by multivariate geostatistics have revealed no significant hydrothermal influence in these deposits (ODADA, 1990a).

The composition of the crusts is strongly influenced by their mineralogy, which is dominated by S-MnO_2, with goethite in one sample (Table 2). Strong associations exist between Co and Ni and S-MnO_2. By contrast, the goethite-rich crust is relatively depleted in these two metals, and unlike any of the other crusts its origin is not so clear. However, hydrogenous goethite-rich ferromanganese oxides have been reported from the Atlantic by MOORBY and CRONAN (1981), and this crust may have formed in a similar manner, i.e. direct precipitation or accumulation of colloidal metal oxides from the water column.

Acknowledgements—I thank the Master and crew of R.R.S. *Shackleton* for the collection of some of the crusts described in this work and P. Bonte and J. L. Reyss of CNRS, Gif-sur-Yvette, France, for additional samples and for helpful discussions. Financial support was received from NERC, UNESCO (Marine Sciences Division) and from the British Council for a research studentship at Imperial College, London.

REFERENCES

APLIN A. C. and D. S. CRONAN (1985) Ferromanganese deposits from the central Pacific Ocean. I. Encrustations from the Line Islands Archipelago. *Geochimica et Cosmochemica Acta*, **49**, 247–436.

AUMENTO F., D. E. LAWRENCE and A. G. PLANT (1968) The ferromanganese pavement on the San Pablo seamount. *Geological Survey of Canada, Professional Paper*, **68**, 32.

CRONAN D. S. (1977) Deep-sea nodules: distribution and geochemistry. In: *Marine manganese deposits*, G. P. GLASBY, editor, Elsevier, Amsterdam, pp. 11–44.

DYMOND J., M. LYLE, B. FINNEY, D. Z. PIPER, K. MURPHY, R. CONRAD and N. PISIAS (1984) Ferromanganese nodules from MANOP Site H, S, and R—Control of mineralogical and chemical composition by multiple accretionary processes. *Geochimica et Cosmochimica Acta*, **48**, 931–949.

FINNEY B., G. R. HEATH and M. LYLE (1984) Growth rates of manganese-rich nodules at MANOP Site H (Eastern North Pacific). *Geochimica et Cosmochimica Acta*, **48**, 911–919.

GODDARD D. A., G. THOMPSON, E. J. W. JONES and H. OKADA (1987) The chemistry and mineralogy of ferromanganese encrustations on rocks from the Sierra Leone Rise, Equatorial Mid-Atlantic Ridge and New England Seamount Chain. *Marine Geology*, **77**, 87–98.

HALBACH P., M. SEGL, D. PUTEANUS and A. MANGINI (1983) Co-fluxes and growth rates in ferromanganese deposits from Central Pacific Seamount areas. *Nature*, **304**, 716–719.

HEIN R. J., F. T. MANHEIM, W. C. SCHWAB and A. S. DAVIS (1985) Ferromanganese crusts from Necker Ridge, Horizon Guyot: geological considerations. *Marine Geology*, **69**, 25–54.

HOFFERT M., A. PERSEIL, R. HEKINIAN, P. CHOUKROUNE, H. D. NEEDHAM, J. FRANCHETEAU and X. LE PICHON (1978) Hydrothermal deposits sampled by diving saucer in transform "A" near 37°N on the mid-Atlantic Ridge, Famous area. *Oceanologica Acta*, **1**, 73–86.

KU T. L. (1977) Rates of accretion. In: *Marine manganese deposits*, G. P. GLASBY, editor, Elsevier, Amsterdam, pp. 249–267.

KU T. L. and W. S. BROECKER (1969) Radiochemical studies on manganese nodules of deep-sea origin. *Deep-Sea Research*, **16**, 625–637.

LYLE M., J. DYMOND and G. R. HEATH (1977) Copper–nickel-enriched ferromanganese nodules and associated crusts from the Bauer Basin, northwest Nazca plate. *Earth and Planetary Science Letters*, **35**, 55–64.

MOORBY S. A. and D. S. CRONAN (1981) The distribution of elements between co-existing phases in some marine ferromanganese oxide deposits. *Geochimica et Cosmochimica Acta*, **45**, 1855–1877.

MOORE W. S., T. L. KU, J. D. MACDOUGALL, V. M. BURNS, R. BURNS, J. DYMOND, M. W. LYLE and D. Z. PIPER (1981) Fluxes of metals to a Mn-nodule. Radiochemical, chemical, structural and mineralogical studies. *Earth and Planetary Science Letters*, **52**, 151–171.

ODADA E. O. (1990a) Geochemistry of sediments from the Romanche Fracture Zone (RFZ), Equatorial Atlantic. *Marine Geology*, **92**, 291–312.

ODADA E. O. (1990b) Geochemistry of ferromanganese crusts from the Romanche Fracture Zones (RFZ), Equatorial Atlantic. In: *Discovery and innovation*, Academy Science Publishers, Vol. 2, No. 2, pp. 153–161.

REYSS J. L., N. LAMAITRE, T. L. KU, V. MARCHIG, J. R. SOUTHON, D. E. NELSON and J. S. VOGEL (1985) Growth of a manganese nodule from Peru Basin: a radiochemical anatomy. *Geochimica et Cosmochimica Acta*, **49**, 2401–2408.

SCOTT M. R., R. B. SCOTT, P. A. RONA, L. W. BUTLER and A. J. NALWALK (1974) Rapidly accumulating manganese deposit from the Median Valley of the mid-Atlantic ridge. *Geophysical Research Letters*, **1**, 335–358.

SEGL M., A. MANGINI, G. BONANI, H. J. HOFMANN, M. NESSI, M. SUTER, W. WOLFLI, G. FRIEDRICH, W. L. PLUGER, A. WIECKOWSKI and J. BEER (1984) ^{10}Be-dating of a manganese crust from central north Pacific and implications for ocean paleocirculation. *Nature*, **309**, 540–543.

THOMPSON J. (1982) A total dissolution method for determination of the alpha-emitting isotopes of uranium and thorium in deep-sea sediments. *Analytica Chimica Acta*, **142**, 259–268.